European Congress on Computational Methods
in Applied Sciences and Engineering (ECCOMAS 2012)
J. Eberhardsteiner et.al. (eds.)
Vienna, Austria, September 10-14, 2012

UPWIND-DIFFERENCE POTENTIALS METHOD FOR CHEMOTAXIS MODELS

Yekaterina Epshteyn[1]

[1]The University of Utah
Department of Mathematics, University of Utah, Salt Lake City, UT, 84112
e-mail: epshteyn@math.utah.edu

Keywords: Simplified Patlak-Keller-Segel chemotaxis model, convection-diffusion-reaction systems, finite difference, finite volume, Difference Potentials methods, Cartesian meshes, complex domains.

Abstract. *We consider here a recently developed upwind-difference potentials method for chemotaxis models [8]. The introduced scheme can be used to approximate problems in complex geometries. The chemotaxis model under consideration is described by a system of two nonlinear PDEs: a convection-diffusion equation for the cell density coupled with a reaction-diffusion equation for the chemoattractant concentration.*

Chemotaxis is an important process in many medical and biological applications, such as bacteria/cell aggregation and pattern formation mechanisms. Modeling of real biomedical problems often has to deal with the complex structure of computational domains.

The upwind-difference potentials method proposed in [8] handles complex domains with the use of only Cartesian meshes, and can be easily employed with fast Poisson solvers. Here, in several numerical tests applied to the simplified Patlak-Keller-Segel model with 'parabolic-elliptic' coupling, we further demonstrate the robustness of the scheme.

1 INTRODUCTION

We consider here one of the most common formulations of the classical Patlak-Keller-Segel system [6]:
Simplified model with the "parabolic-elliptic" coupling (obtained in the assumption that concentration c changes over much smaller time scales), which can be written in the dimensionless form as well

$$\begin{cases} \rho_t + \nabla \cdot (\chi \rho \nabla c) = \Delta \rho, \\ \Delta c - c + \rho = 0, \end{cases} \qquad (x, y) \in \Omega, t > 0, \tag{1}$$

subject to the Neumann boundary conditions:

$$\nabla \rho \cdot \mathbf{n} = \nabla c \cdot \mathbf{n} = 0, \quad (x, y) \in \partial\Omega. \tag{2}$$

Here, $\rho(x, y, t)$ is the cell density, $c(x, y, t)$ is the chemoattractant concentration, χ is a chemotactic sensitivity constant, Ω is a bounded domain in $\mathbb{R}^2$, $\partial\Omega$ is its boundary, and $\mathbf{n}$ is a unit normal vector.
Chemotaxis is the process by which cellular motion occurs in response to an external stimulus, usually a chemical one. It is an important mechanism in many medical and biological applications, including bacteria/cell aggregation and pattern formation mechanisms, as well as tumor growth. Chemotaxis models are usually highly nonlinear due to the density dependent cross diffusion term (attracting force) that models chemotactic behavior, and hence any realistic chemotaxis model is too difficult to solve analytically. Therefore, development of accurate and efficient numerical methods is crucial for the modeling and analysis of chemotaxis systems. Furthermore, a common property of all existing chemotaxis systems is their ability to model a concentration phenomenon that mathematically results in rapid growth of solutions in small neighborhoods of concentration points/curves. The solutions may blow up or may exhibit a very singular, spiky behavior. This blow-up represents a mathematical description of a cell concentration phenomenon that occurs in real biological systems, see, e.g., [1, 2, 3, 4, 7, 11].

There exists an extensive literature about chemotaxis models, their mathematical analysis and numerical approximation. A detailed overview can be found for example in [8].

While modeling real biomedical problems, one often has to deal with the complex structure of the computational domains. Thus, there is a need for accurate, fast, and computationally efficient numerical methods for different chemotaxis models that can handle arbitrary geometries. In this work we consider and test further the upwind-difference potentials method [8] which can handle complex geometry without the use of unstructured meshes (with the consideration of only Cartesian grids) and that can be employed with fast Poisson solvers. This method combines the simplicity of the positivity-preserving upwind scheme for chemotaxis models on Cartesian meshes [5] with the flexibility of the Difference Potentials method [13].

The paper is organized as follows. First, in Section 2 we give a brief overview of the upwind-difference potentials method and steps of the algorithm. Secondly, we illustrate the performance of the proposed scheme for simplified Patlak-Keller-Segel model in several numerical experiments in Section 3. Some concluding remarks are given in Section 4.

2 OVERVIEW OF THE SECOND ORDER UPWIND-DIFFERENCE POTENTIALS METHOD FOR 2D CHEMOTAXIS MODELS

In this section, we will review the main ideas of the second-order upwind-difference potentials method [8]. The scheme is based on:

- *Second order positivity preserving upwind method on Cartesian meshes [5, 8]*

- *and Difference Potentials Method (DPM) [12, 13]*

2.1 Positivity preserving upwind scheme on cartesian mesh - a brief overview

We assume here that we consider the Patlak-Keller-Segel system (1) in a square domain $D \subset \mathbb{R}^2$.
Let us introduce a Cartesian mesh for domain D consisting of the uniform cells $D_{j,k} := [x_{j-\frac{1}{2}}, x_{j+\frac{1}{2}}] \times [y_{k-\frac{1}{2}}, y_{k+\frac{1}{2}}]$ of the size $\Delta x \Delta y$ centered at the point $(x_j := j\Delta x, y_k := k\Delta y)$. Let us also define a five-point stencil $N_{j,k}$ with center placed at (x_j, y_k) to be the set of the following points: $N_{j,k} := \{(x_j, y_k), (x_{j\pm1}, y_k), (x_j, y_{k\pm1})\}$.

The fully discrete positivity preserving upwind scheme for the Patlak-Keller-Segel system (1) is given below:

$$\begin{cases} \Delta_{j,k}\bar{\rho}^{i+1} - m\bar{\rho}^{i+1}_{j,k} = g^{\rho}_{j,k}, \quad (x_j, y_k) \in M, \\ \Delta_{j,k}c^{i+1} - c^{i+1}_{j,k} = g^{c}_{j,k}, \quad (x_j, y_k) \in M, \end{cases} \tag{3}$$

where the unknowns for which we will be solving at the time level t^{i+1} are $(\bar{\rho}^{i+1}, c^{i+1})$.
The computed quantities are the cell averages of the density ρ, $\bar{\rho}_{j,k}(t) \approx \frac{1}{\Delta x \Delta y}\int\int_{D^0_{j,k}} \rho(x, y, t)\Delta x \Delta y$ and the point values $c_{j,k}(t) \approx c(x_j, y_k, t)$. Here, we denote $\bar{\rho}^i_{j,k}$ is the computed $\bar{\rho}_{j,k}(t^i)$ at the discrete time level $t^i := i\Delta t$ with time step Δt and $c^i_{j,k}$ is the computed $c_{j,k}(t^i)$.

$\Delta_{j,k}$ denotes the discrete Laplacian obtained using second order central difference formulas for the x and y variables and $m := \frac{1}{\Delta t}$.
The right-hand side for the density equation is evaluated at the previous time level t^i and will be denoted by $g^{\rho}_{j,k}$ for the brevity of the exposition:

$$g^{\rho}_{j,k} := -m\bar{\rho}^i_{j,k} + \frac{H^x_{j+\frac{1}{2},k} - H^x_{j-\frac{1}{2},k}}{\Delta x} + \frac{H^y_{j,k+\frac{1}{2}} - H^y_{j,k-\frac{1}{2}}}{\Delta y}. \tag{4}$$

Here,

$$H^x_{j+\frac{1}{2},k} = \chi\rho^i_{j+\frac{1}{2},k}\Big(\frac{c^i_{j+1,k} - c^i_{j,k}}{\Delta x}\Big), \quad H^y_{j,k+\frac{1}{2}} = \chi\rho^i_{j,k+\frac{1}{2}}\Big(\frac{c^i_{j,k+1} - c^i_{j,k}}{\Delta y}\Big) \tag{5}$$

are the upwind numerical fluxes with

$$\rho^i_{j+\frac{1}{2},k} = \begin{cases} \widetilde{\rho}^i(x_{j+\frac{1}{2}} - 0, y_k) \text{ if } \Big(\frac{c^i_{j+1,k} - c^i_{j,k}}{\Delta x}\Big) > 0, \\ \widetilde{\rho}^i(x_{j+\frac{1}{2}} + 0, y_k), \text{ otherwise} \end{cases}$$

Similarly,

$$\rho^i_{j,k+\frac{1}{2}} = \begin{cases} \widetilde{\rho}^i(x_j, y_{k+\frac{1}{2}} - 0) \text{ if } \Big(\frac{c^i_{j,k+1} - c^i_{j,k}}{\Delta y}\Big) > 0, \\ \widetilde{\rho}^i(x_j, y_{k+\frac{1}{2}} + 0), \text{ otherwise} \end{cases}$$

Here,

$$\widetilde{\rho}^i(x, y) = \bar{\rho}^i_{j,k} + (\rho^i_x)_{j,k}(x - x_j) + (\rho^i_y)_{j,k}(y - y_k), \quad (x, y) \in D^0_{j,k} \tag{6}$$

is the piecewise linear reconstruction with the slopes $(\rho^i_x)_{j,k}$ and $(\rho^i_y)_{j,k}$ calculated using the minmod limiter,

$$(\rho^i_x)_{j,k} = minmod\Big(2\frac{\bar{\rho}^i_{j+1,k} - \bar{\rho}^i_{j,k}}{\Delta x}, \frac{\bar{\rho}^i_{j+1,k} - \bar{\rho}^i_{j-1,k}}{2\Delta x}, 2\frac{\bar{\rho}^i_{j,k} - \bar{\rho}^i_{j-1,k}}{\Delta x}\Big)$$

and

$$(\rho_y^i)_{j,k} = minmod\Big(2\frac{\bar{\rho}^i_{j,k+1} - \bar{\rho}^i_{j,k}}{\Delta y}, \frac{\bar{\rho}^i_{j,k+1} - \bar{\rho}^i_{j,k-1}}{2\Delta y}, 2\frac{\bar{\rho}^i_{j,k} - \bar{\rho}^i_{j,k-1}}{\Delta y}\Big).$$

The minmod function is defined by

$$minmod(z_1, z_2, ..., z_p) := \begin{cases} min(z_1, z_2, ..., z_p), \text{ if } z_i > 0 \quad \forall i = 1, ..., p, \\ max(z_1, z_2, ..., z_p), \text{ if } z_i < 0 \quad \forall i = 1, ..., p, \\ 0, \text{ otherwise} \end{cases}$$

The right-hand side for the concentration equation $g^c_{j,k}$ is

$$g^c_{j,k} := -\bar{\rho}^i_{j,k} \tag{7}$$

The scheme (3) is positivity preserving. The more detailed discussion about this scheme can be found for example in [8].

2.2 Difference potentials - a brief overview

Let us now briefly review the Difference Potentials idea ([8]). We are concerned here with the Patlak-Keller-Segel system (1) in some domain Ω - an arbitrary bounded domain in $\mathbb{R}^2$ with the boundary $\partial\Omega$.

We introduce the auxiliary difference problem. Let us place the original domain Ω in the auxiliary domain $D^0 \subset \mathbb{R}^2$. The choice of the domain D^0 should be convenient for computations so we will choose it to be a square, and we will introduce a Cartesian mesh for D^0 consisting of the uniform cells $D^0_{j,k} := [x_{j-\frac{1}{2}}, x_{j+\frac{1}{2}}] \times [y_{k-\frac{1}{2}}, y_{k+\frac{1}{2}}]$ of the size $\Delta x \Delta y$ centered at the point $(x_j := j\Delta x, y_k := k\Delta y)$. Let us define a five-point stencil $N_{j,k}$ with its center placed at (x_j, y_k) to be the set of the following points: $N_{j,k} := \{(x_j, y_k), (x_{j\pm1}, y_k), (x_j, y_{k\pm1})\}$.
In addition, let us also introduce point sets $M := M^\rho = M^c := (x_j, y_k) \in \Omega$ - the sets of all the points (x_j, y_k) that belong to the interior of the original domain Ω. We now define $N := N^\rho = N^c = \{\bigcup_{j,k} N_{j,k} | (x_j, y_k) \in M\}$- the set of all points covered by five-point stencils when center point (x_j, y_k) of the stencil goes through all the points of the set M.
Let us remark, that points in the set N will be both inside and outside of the original domain Ω. Also, let us mention that index ρ and c were used to emphasize that in general we can have different grids for the numerical approximation of the density and concentration but in this work we consider the same grid.
Now, let us introduce the grid boundaries $\gamma_{ex} := \gamma^\rho_{ex} = \gamma^c_{ex} := N \backslash M$- exterior grid boundary layer for domain Ω, $\gamma_{in} := \gamma^\rho_{in} = \gamma^c_{in} := \{(x_j, y_k) | (x_j, y_k) \in M : N_{j,k} \not\subset M\}$ - interior grid boundary layer for domain Ω and define $\gamma := \gamma_{ex} \cup \gamma_{in}$ - a narrow set of nodes which surrounds the continuous boundary $\partial\Omega$, Fig. (2.2) .
Let us also construct the auxiliary set $M^1 := M^{1,\rho} = M^{1,c}$ by completing the set N to a rectangle and adding one extra layer of grid points to each side of the rectangle, hence $N \subset M^1$. Also, as before, define $N^1 := N^{1,\rho} = N^{1,c} = \{\cup_{j,k} N_{j,k} | (x_j, y_k) \in M^1\}$ and finally, let us introduce $\gamma^1 := \gamma^{1,\rho} = \gamma^{1,c} = N^1 \backslash M^1$.

Based on a scheme (3), we will formulate now a *General Auxiliary Problem:*
For the given grid functions g^1 and g^2, find the solution of the scheme (f^1, f^2) such that:

$$\Delta_{j,k} f^1 - m f^1_{j,k} = g^1_{j,k}, \quad (x_j, y_k) \in M_1, \tag{8}$$

$$f^1_{j,k} = 0, \quad (x_j, y_k) \in \gamma^1 \tag{9}$$

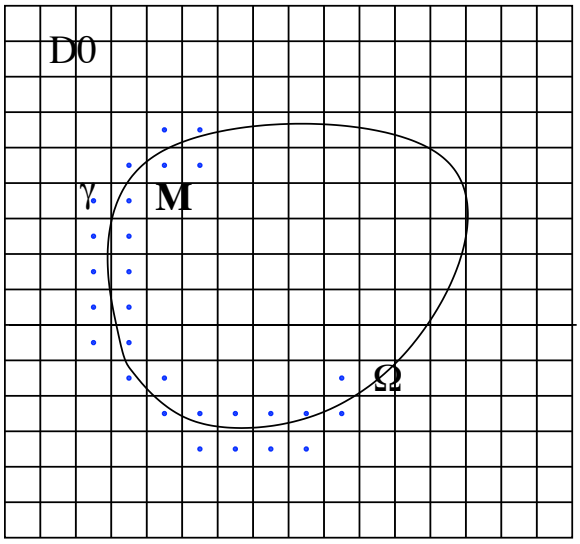

Figure 1: Example (a sketch) of the auxiliary domain D^0, original domain Ω; the example of some points (x_j, y_k)(-centers of the grid cells) in the set γ: the points which are outside Ω are from γ_{ex}, the points which are inside Ω are from $\gamma_{in} \in M$

$$\Delta_{j,k} f^2 - f^2_{j,k} = g^2_{j,k}, \quad (x_j, y_k) \in M_1, \tag{10}$$

$$f^2_{j,k} = 0, \quad (x_j, y_k) \in \gamma^1 \tag{11}$$

We note that the *General Auxiliary Problem* (8)-(11) is well defined for any right hand side $g^1_{j,k}, g^2_{j,k}$ - it has a unique solution (f^1, f^2) defined on the set N^1.
Also, it can be noted that the solution of (8)-(11) can be efficiently computed using the Fast Fourier Transform (FFT) with the appropriate choice of the auxiliary set M^1.
Next, we denote by

$$\mathbf{f} := (f^{\bar{\rho}}, f^c) \tag{12}$$

the solution (f^1, f^2) of the auxiliary problem (8)-(11) when the right hand-sides are defined as

$$g^1_{j,k} := \begin{cases} g^\rho_{j,k}, & (x_j, y_k) \in M, \\ 0, & (x_j, y_k) \in M^1 \backslash M \end{cases} \tag{13}$$

and

$$g^2_{j,k} := \begin{cases} g^c_{j,k}, & (x_j, y_k) \in M, \\ 0, & (x_j, y_k) \in M^1 \backslash M \end{cases} \tag{14}$$

where $g^\rho_{j,k}$ and $g^c_{j,k}$ are given in (4) and (7).

We now introduce a linear space V_γ of all grid functions denoted by $\mathbf{v}_\gamma := (\bar{\rho}^\gamma, c^\gamma)$ defined on γ, similar to [12, 13]. We will extend by zero the value of $\mathbf{v}_\gamma$ to other points of the grid D^0.

Let us recall that, *Difference Potential* [12, 13] with the given density $\mathbf{v}_\gamma$ is the grid function $\mathbf{u} = (u_{\bar{\rho}}, u_c) := \mathbf{P}\mathbf{v}_\gamma$ which coincides with the solution of (8)-(11) with the right hand-side defined as follows:

$$g^1_{j,k} := \begin{cases} 0, & (x_j, y_k) \in M, \\ \Delta_{j,k}\bar{\rho}^\gamma - m\bar{\rho}^\gamma_{j,k}, & (x_j, y_k) \in M^1 \backslash M \end{cases} \tag{15}$$

and

$$g^2_{j,k} := \begin{cases} 0, & (x_j, y_k) \in M, \\ \Delta_{j,k} c^\gamma - c^\gamma_{j,k}, & (x_j, y_k) \in M^1 \backslash M \end{cases} \tag{16}$$

Here, $\mathbf{P}$ denotes the operator which constructs difference potential $\mathbf{u} = \mathbf{P}\mathbf{v}_\gamma$ from the given density $\mathbf{v}_\gamma \in V_\gamma$. The operator $\mathbf{P}$ is the linear operator of the density $\mathbf{v}_\gamma$ which can be easily constructed [8, 13].

Next, let us recall [8, 12, 13] and define another operator $\mathbf{P}_\gamma : V_\gamma \to V_\gamma$ which is defined as the trace (or restriction) of the Difference Potential $\mathbf{P}\mathbf{v}_\gamma$ on the grid boundary γ: $\mathbf{P}_\gamma := Tr_\gamma \mathbf{P}\mathbf{v}_\gamma = \mathbf{P}\mathbf{v}_\gamma|_\gamma$.
Let us now state the main theorem for our scheme [8].

Theorem 2.1 *At each time level density $\mathbf{v}_\gamma = (\bar{\rho}^\gamma, c^\gamma) \in V_\gamma$ is the trace of some solution $\mathbf{u}^{\bar{\rho}\mathbf{c}} := (\bar{\rho}, c)$ to the upwind scheme (3): $\mathbf{v}_\gamma = Tr_\gamma \mathbf{u}^{\bar{\rho}\mathbf{c}}$, if and only if we have*

$$\mathbf{v}_\gamma = \mathbf{P}_\gamma \mathbf{v}_\gamma + \mathbf{f}_\gamma, \tag{17}$$

where $\mathbf{f}_\gamma = \mathbf{Tr}_\gamma \mathbf{f}$ and f is defined in (12).

Hence, this theorem implies that the unique solution $\mathbf{u}^{\mathbf{pks}} := (\bar{\rho}, c)$ to problem (3), subject to the boundary conditions on $\partial\Omega$, is the unique solution of the following problem (18) (and vice versa: the unique solution of the problem (18) is the unique solution to the problem (3) subject to the corresponding boundary conditions):
Algorithm

1. At time level t^{i+1} find the solution $\mathbf{f} = (f^{\bar{\rho}}, f^c)$ of the auxiliary problem (8)-(11), (13)-(14)

2. Solve system of boundary equations for the unknown $\mathbf{v}_\gamma$ with the imposed boundary conditions:
$$\mathbf{v}_\gamma = P_\gamma \mathbf{v}_\gamma + \mathbf{f}_\gamma, \quad l(\mathbf{P}\mathbf{v}_\gamma + \mathbf{f}) = \psi \tag{18}$$

3. Construct difference potential $P\mathbf{v}_\gamma$ with the obtained density $\mathbf{v}_\gamma$

4. At each time level t^{i+1}: $\mathbf{u}^{\mathbf{pks}} = P\mathbf{v}_\gamma + \mathbf{f}$,

where $l(\mathbf{P}\mathbf{v}_\gamma + \mathbf{f}) = \psi$ is the proper approximation at the points of set γ of the zero Neumann boundary conditions for $(\bar{\rho}, c)$. This approximation can be obtained, for example, using either an interpolation idea to approximate $\frac{\partial \bar{\rho}}{\partial n}$ and $\frac{\partial c}{\partial n}$ at some points in set γ, or by using a spectral approximation approach to approximate the boundary conditions [8].

3 NUMERICAL EXAMPLES: VALIDATION OF THE UPWIND-DIFFERENCE POTENTIALS METHOD ON A SIMPLIFIED CHEMOTAXIS MODEL WITH RADIALLY SYMMETRIC INITIAL DATA IN A CIRCLE

In this section, similar to the tests in [8], we demonstrate the performance of the upwind-difference potentials scheme for the simplified Patlak-Keller-Segel chemotaxis model (1). In the numerical experiments we used the upwind scheme (3) with the minmod limiter with $\theta = 2$.

We consider the Patlak-Keller-Segel chemotaxis problem (1) -(2) in a circular domain $x^2 + y^2 = 0.25$ with the radially symmetric initial data:

$$\rho(x, y, 0) = \rho_0 e^{-100(x^2+y^2)}, \quad c(x, y, 0) = 0.5\rho_0 e^{-50(x^2+y^2)}, \tag{19}$$

where ρ_0 is the constant which will be specified later.

It has been proven (see, for example overview [9, 10]) that the solution to Patlak-Keller-Segel chemotaxis model with 'parabolic-elliptic' coupling in $\Omega \in \mathbb{R}^2$:

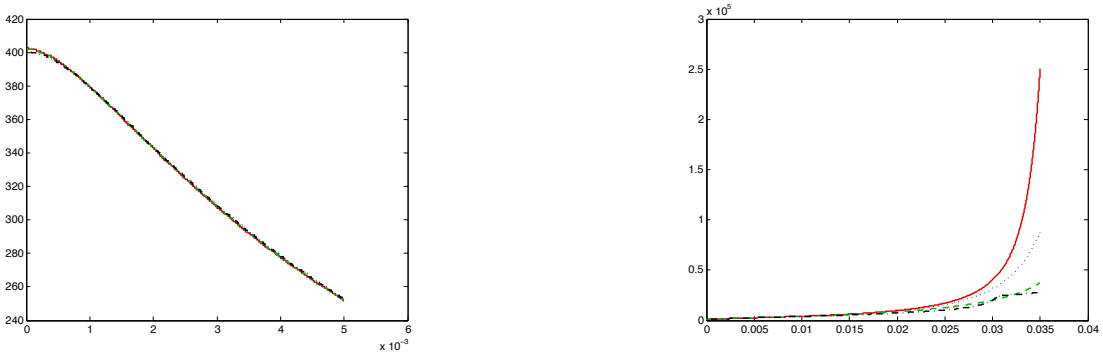

Figure 2: Plots of $\rho_{\max}(t)$ - the evolution of the maximum value of the density ρ with time: left plot is for the case 1 with $\rho_0 = 400$ and the right plot is for the case 2 with $\rho_0 = 850$. Red solid line is $\rho_{\max}(t)$ computed on mesh 507×507; dotted blue is for 251×251; green dashed is for 123×123, and dark blue dash dotted is for 59×59

1. exists globally in time if the initial mass is $\int_\Omega \rho(x, y, 0)dxdy < 8\pi$
2. is expected to blow up if the initial mass is $8\pi < \int_\Omega \rho(x, y, 0)dxdy$

We validate our scheme below by checking numerically properties (1) and (2).

For case (1) we set $\rho_0 = 400$ (plot of the initial data, Fig. 4) and we illustrate numerically (left plot on Fig. 2) similar to the test for Patlak-Keller-Segel chemotaxis model with 'parabolic-parabolic' coupling [8] that solution exists globally in time. However, compared to the full model [8], the simplified model produces different type of evolution of the maximum value of the density ρ with time.

For the case (2) we consider $\rho_0 = 850$ (plot of the initial data, Fig. 5) and we again show that similar to the test with full Patlak-Keller-Segel system with 'parabolic-parabolic' coupling [8], the proposed scheme will break the symmetry and the solution will approach the blow up (right plot on Fig. 2) and will blow up at the center of the circular domain as expected by the theory (Fig. 3 - density ρ at time around the blow-up time). However, compared to the similar test in [8] for the full chemotaxis model, it takes much longer time for the density ρ to approach the blow up.

In Fig. 2 we plot the evolution of the maximum value of the density ρ with time

$$\rho_{\max}(t) := \max_{(x,y)} \rho(x, y, t)$$

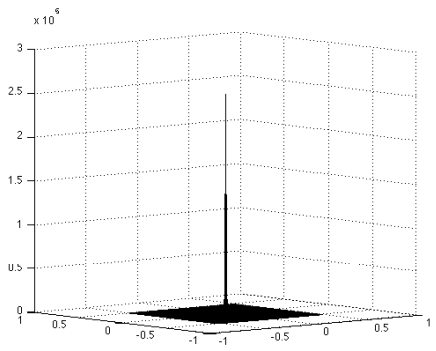

Figure 3: Plot of the density ρ for the case 2 with $\rho_0 = 850$ at time around the blow up time $t \approx 0.035$. The solution is computed on mesh 507×507

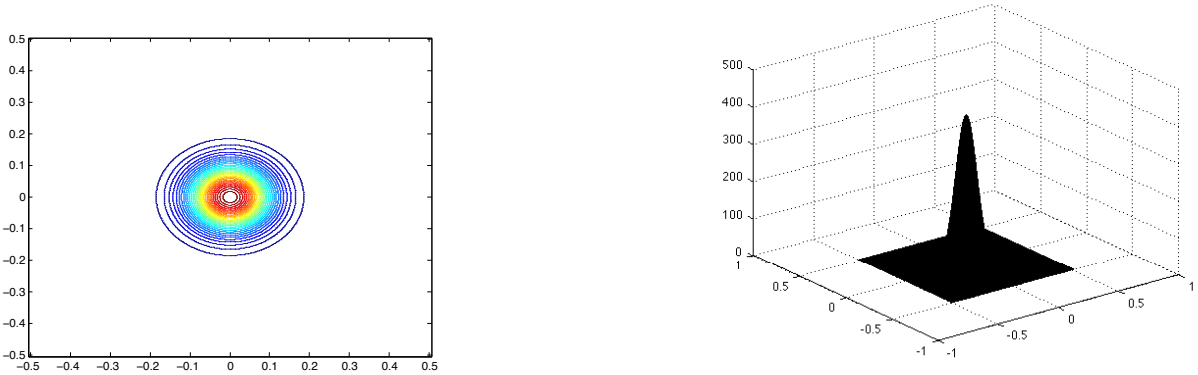

Figure 4: Plot of the initial data $\rho(x, y, 0)$ with initial mass below 4π

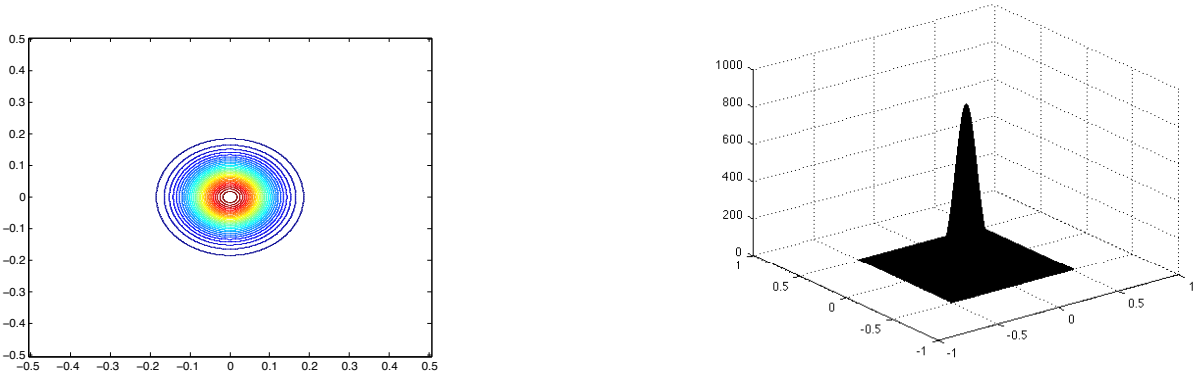

Figure 5: Plot of the initial data $\rho(x, y, 0)$ with initial mass above 8π

on four different meshes - mesh 59×59, 123×123, 251×251 and 507×507.

4 CONCLUSIONS

We consider here a recently developed upwind-difference potentials scheme for chemotaxis models and closely related problems in physics and biology [8]. The scheme can handle complex computational domains with the use of only Cartesian grids, and can be easily employed with fast Poisson solvers. The proposed method combines the simplicity of a positivity-preserving upwind scheme on Cartesian meshes with the flexibility of the Difference Potentials method. Further numerical experiments for a simplified Patlak-Keller-Segel chemotaxis model are presented to illustrate robustness of the upwind-difference potentials scheme.

Acknowledgment: The author is deeply grateful to Viktor Ryaben'kii for his attention to this work, helpful discussions and encouragements. The research is supported in part by the National Science Foundation Grant # DMS-1112984.

REFERENCES

[1] J. Adler. Chemotaxis in bacteria. *Ann. Rev. Biochem.*, 44:341–356, 1975.

[2] J.T. Bonner. *The cellular slime molds*. Princeton University Press, Princeton, New Jersey, 2nd edition, 1967.

[3] E.O. Budrene and H.C. Berg. Complex patterns formed by motile cells of escherichia coli. *Nature*, 349:630–633, 1991.

[4] E.O. Budrene and H.C. Berg. Dynamics of formation of symmetrical patterns by chemotactic bacteria. *Nature*, 376:49–53, 1995.

[5] A. Chertock, Y. Epshteyn, and A. Kurganov. High-order finite-difference and finite-volume methods for chemotaxis models. 2010. in preparation.

[6] S. Childress and J.K. Percus. Nonlinear aspects of chemotaxis. *Math. Biosc.*, 56:217–237, 1981.

[7] M.H. Cohen and A. Robertson. Wave propagation in the early stages of aggregation of cellular slime molds. *J. Theor. Biol.*, 31:101–118, 1971.

[8] Yekaterina Epshteyn. Upwind-difference potentials method for Patlak-Keller-Segel chemotaxis model. *Journal of Scientific Computing*, pages 1–25. 10.1007/s10915-012-9599-2.

[9] D. Horstmann. From 1970 until now: The Keller-Segel model in chemotaxis and its consequences i. *Jahresber. DMV*, 105:103–165, 2003.

[10] D. Horstmann. From 1970 until now: The Keller-Segel model in chemotaxis and its consequences ii. *Jahresber. DMV*, 106:51–69, 2004.

[11] L.M. Prescott, J.P. Harley, and D.A. Klein. *Microbiology*. Wm. C. Brown Publishers, Chicago, London, 3rd edition, 1996.

[12] V. S. Ryaben′kiĭ, V. I. Turchaninov, and E. Yu. Èpshteĭn. An algorithm composition scheme for problems in composite domains based on the method of difference potentials. *Zh. Vychisl. Mat. Mat. Fiz.*, 46(10):1853–1870, 2006.

[13] V.S. Ryaben'kii. Method of difference potentials and its applications. *Springer-Verlag*, 2001.